UNEXPECTED COMPLEXITY OF EVERYDAY MANUAL BEHAVIORS

Yuke Yan[1], James G. Goodman[1], & Sliman J. Bensmaia[1,2]

[1]Committee on Computational Neuroscience, University of Chicago, Chicago, IL
[2]Department of Organismal Biology and Anatomy, University of Chicago, Chicago, IL

ACKNOWLEDGMENTS
We would like to thank Dalton Moore for help with experimental design and data collection. We would like to thank Matt Kaufman for help with the title. This work was supported by NINDS grant R01 NS082865.

ABSTRACT

How does the brain control an effector as complex and versatile as the hand? One possibility is that the neural control of the hand is simplified by limiting the number of achievable hand postures. Indeed, hand kinematics can be largely accounted for within a small subspace. This oft replicated finding has been interpreted as evidence that hand postures are confined to this subspace and that leaving it volitionally is impossible. A prediction from this hypothesis is that measured hand movements that fall outside of this subspace reflect motor or measurement noise. To address this question, we track hand postures of human participants as they perform three tasks – grasping, typing, and signing in American Sign Language. We then apply a standard dimensionality reduction technique – principal components analysis – and replicate the finding that hand movements can be largely described within a much reduced subspace. However, we show that kinematic dimensions that fall outside of this subspace are highly structured and task dependent, suggesting that they too are under volitional control. Moreover, we find that the hand kinematics of monkeys performing a grasping task also occupy a high-dimensional space as do the underlying neuronal representations in primary motor cortex. We conclude that hand control occupies a high dimensional space and propose that the complexity of hand movements is well within the scope of the brain's computational power.

INTRODUCTION

From picking up a coffee cup to playing the piano, humans can engage in a wide range of manual behaviors, highlighting the staggering flexibility of the hand: The 27 bones and 39 muscles give rise to more than 20 degrees of freedom (DOF) of movement [1,2]. This versatility is also mediated by a sophisticated neural system: the hand is one of the most densely innervated regions of the human body [3] and the hand representation in sensorimotor cortex is disproportionately large [4]. Additionally, although primate motor cortex lacks a clear somatotopic organization [5], it nonetheless seems to contain a specialized module for hand control [6].

The complexity of the hand has called into question whether the central nervous system (CNS) can fluidly control such a complex effector [7,8]. An appealing hypothesis is that hand postures – which in theory can exist over 20 or more degrees of freedom – are reduced to a lower dimensional manifold to simplify the control problem [7–9]. Instead of spanning the space afforded by every DOF, hand control relies on a set of synergies that are combined to give rise to manual behaviors. Broadly defined, a synergy is a set of muscle activations or joint movements that are recruited in tandem, rather than individually [10]. This restriction of volitional movements of the hand to combinations of a small number of synergies would then help the CNS achieve fluid manual behaviors. To date, many studies have looked for hand synergies in different movement contexts, with a mixture of evidence for and against the notion that the CNS indeed constrains hand movements to a limited basis set [9–18].

The most compelling evidence for synergies stems from analysis of hand kinematics or of the muscle activations that drive them, which seem to occupy a lower dimensional manifold than might be expected from counting the DOFs. Indeed, principal component analysis (PCA) of kinematics of muscle activations reveals that a small number of principal components (PCs) account for most of the variance in the movements, typically measured for a single behavior (e.g. grasping, playing piano,

typing)[11,12,19–23]. The more or less explicit assumption underlying the interpretation of this dimensionality reduction is that high-variance principal components (PCs) – the synergies – are under volitional control whereas low-variance PCs reflect motor or measurement noise. Another possibility, however, is that the exquisite control of the hand is mediated by high dimensional sensorimotor signals,

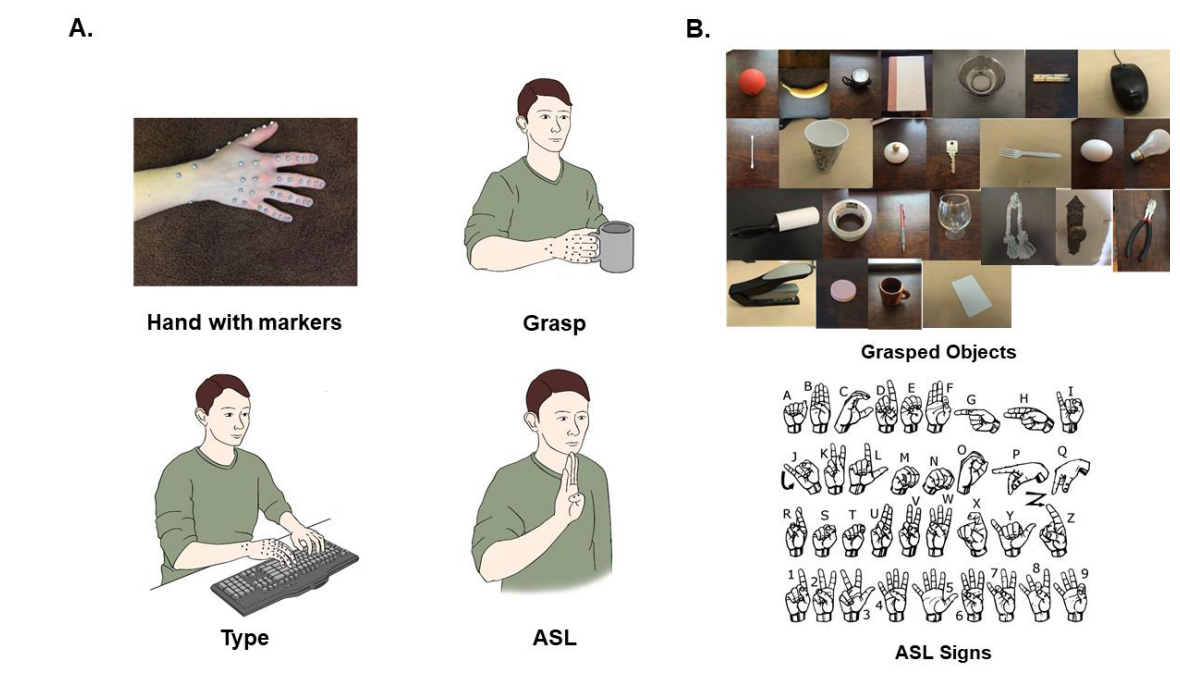

Figure 1. Experimental design. A| Subjects performed three different manual tasks with reflective markers placed on their right hand: Grasping objects, signing in American Sign Language, and typing on keyboard. Infrared cameras tracked the 3D trajectories of the markers and joint angles were calculated from them. B| Grasped objects and ASL signs.

and that low-variance PCs are critical to achieving precise hand postures.

The aim of the present study is to assess whether hand movements exist in a manifold whose dimensionality is lower than its theoretical value, defined by the hand's DOFs. To this end, we have human participants perform three manual behaviors – grasping, signing letters in American Sign Language, and typing on a keyboard – while we track their hand kinematics. We then assess the degree to which low-variance PCs are structured by assessing the degree to which they carry information about the manual behavior. For example, humans and non-human primates precisely preshape their hands when grasping objects. Objects can thus be classified on the basis of the kinematics they evoke during grasping even before contact. If low-variance PCs indeed reflect noise, they should bear no systematic relationship with the object to be grasped. However, if low-variance PCs reflect subtle but volitionally controlled adjustments of hand posture to better preshape to the object, these should also be highly object specific. We also investigate the degree to which the space of hand movements depends on the behavior. Specifically, how similar are the kinematic spaces in the three manual behaviors?

METHODS

Human kinematics

Experimental design

All procedures were approved by the institutional review board (IRB) of the University of Chicago. Eight right-handed adult subjects between the ages of 21 to 40 participated in the experiment. During the experiment, subjects were instructed to perform three different types of manual tasks: Grasping objects, typing on a keyboard, and singing letters in American Sign Language (ASL) (**Figure 1A)**. All eight subject performed the grasping and typing tasks and three subjects – who had prior knowledge of ASL – performed the signing task. Grasping and ASL involved only the subjects' right hand and only the right hand was tracked during typing.

In the grasping tasks, subjects began each trial by resting their right hand on a table in front of them. The experimenter then placed an object at the center of the table and subjects grasped the object with their right hands, lifted it, and held it up for approximately 1 second before replacing the object on the table and moving their hand back to the starting position. This procedure was repeated five times for each object. Twenty five objects, varying in size, shape, and orientation were used to elicit 30 distinct grasps (some objects could be grasped in several ways; for example, a light bulb can be grasped by the stem or by the bulb, **Figure 1B**).

In the typing task, subjects used a keyboard to type two 300-word passages, each divided into four paragraphs of approximately equal length (**Supplementary Figure 3**). The first passage was a "word salad" designed to maximize right hand movements: All words were anagrams of the letters to the right of the "Y-G-V" boundary (inclusive) on a QWERTY keyboard. The words were arranged in written English syntax with common punctuations but did not follow any grammatical rules or carry any meaning. The second passage, taken from the Wikipedia page of neocortex (https://en.wikipedia.org/wiki/Neocortex), comprised approximately equal distributions of letters on both halves of the keyboard.

In the ASL task subjects started at the same position as in the grasping task. On each trial, subjects signed an ASL sign – one of the 26 letters of the alphabet or a number from 1 to 10 – and repeated it five times.

Measurement and pre-processing

Forty one infrared-reflective markers (hemisphere shape, 4-mm diameter) were placed on the right hand of each subject, with two markers covering each finger joint, two on the ulnar and one on the radial bone of the forearm (**Figure 1A**). Thirteen infrared cameras (8MP resolution, 250Hz)(Vantage, VICON, Los Angeles, CA) fixed to wall mounts and camera stands tracked the 3D trajectories of each marker, each of which was then labeled based on its respective joint using Vicon Nexus Software (VICON, Los Angeles, CA). We used a musculoskeletal model of the human forearm taken from the full-body model [24] in OpenSim [25], which comprises 29 degrees of freedom, including all joints on the human hand and three wrist movement parameters. Scaling the model to each subject, we then performed inverse kinematics to estimate time-varying joint angles using least-square optimization [25].

Monkey kinematics and neurophysiology

Surgery and experimental design

All animal procedures conformed to the rules and regulations of the University of Chicago Animal Care and Use Committee (IACUC). Surgical and neurophysiological procedures have been previously described [26] and are only summarized here. In brief, two Rhesus Macaques (ae: 6 to 15 years; weight: 8 to 11 kg) were implanted with electrode arrays in the hand representation of sensorimotor cortex: Monkey 1 was implanted with one Utah electrode array (UEAs, Blackrock Microsystems, Inc., Salt Lake City, UT) in primary motor cortex and Monkey 2 was implanted with a semi-chronic microdrive electrode array (SC96, Gray Matter Research, Bozeman, MT), covering large swaths of primary motor and somatosensory cortex.

Animals performed a grasping task similar to that described above for human subjects (25 objects, 35 distinct grasping postures) but without the reaching component. On each trial, a robotic arm (MELFA RV-1A, Mitsubishi Electric, Tokyo, Japan) brought an object to the animal's stationary hand and the animal preshaped its hand to grasp it. After grasp, animals maintained contact with the object for 1 to 3 seconds, after which the robotic hand retracted. In a given experiment session, each object was presented eight to eleven times. Thirty-one Infrared-reflective markers were placed on the bony landmarks on the joints of the hand and forearm and their three-dimensional positions were tracked by a 14-camera motion tracking system (MX T-Series, VICON, Los Angeles, CA) while we recorded the responses evoked in primary motor cortex.

Pre-processing of kinematics and neuronal data

Inverse kinematics were calculated using time=varying marker positions and a musculoskeletal model of the human arm (https://simtk.org/projects/ulb_project) [27–33] implemented in Opensim (https://simtk.org/frs/index.php?group_id=91) [25]. The model was modified to include three rotational degrees of freedom of the first and fifth carpo-metacarpal joints to permit reconstructions of oppositional movements of these digits. In total, we reconstructed the time-varying angles of 29 degrees of freedom, including all movement parameters of the hand and three of the wrist.

Analysis

We included in the analysis kinematics and neuronal responses obtained prior to contact with the object.

Principal components analysis & cross-projection similarity

Kinematic synergies have been identified using principal components analysis (PCA), which expresses hand postural trajectories in terms of a set of orthogonal bases, each of which consists of correlated joint trajectories. We applied PCA to kinematics obtained from humans and monkeys and to neuronal responses obtained from monkeys [34]. To compare PC subspaces across subjects or tasks, we computed the cross-projection similarity [11]. For this, we first calculated the total variance accounted for by the first N PCs of one group (V1). Then, we projected the scores of the first N PCs of that group onto the first N PCs of a second group and computed the total variance explained in group 1 by the

projection onto group 2 PCs (V2). Finally, we computed the ratio V2/V1. The ratio V2/V1 approaches 1 to the extent that the second subspace resembles the first. To compare kinematic subspaces across tasks, we performed a PCA on the data from each task pooled across subjects and computed the cross-projection similarity using the first 10 PCs (~95% variance explained).

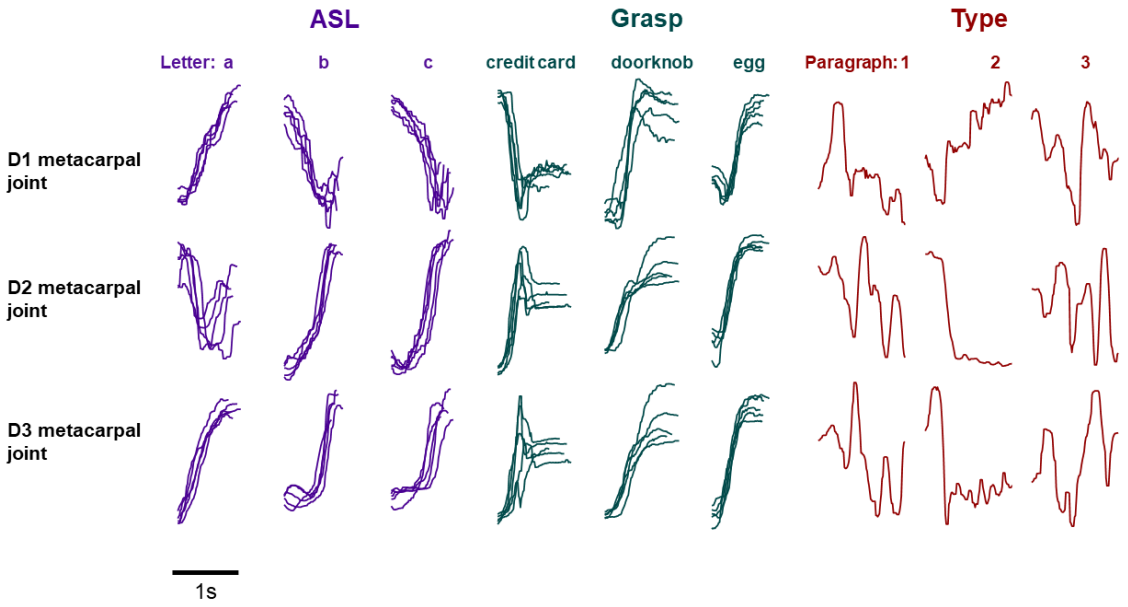

Figure 2. Example kinematic traces. Joint kinematics (metacarpophalangeal joints flexion of digits 1 to 3) evoked during the three manual tasks: ASL, grasp and typing. For ASL and grasp, the kinematics evoked during grasping of three different objects or signing of three ASL signs are shown for five trials. For typing, the initial 1-second epoch of typing three different paragraphs is shown.

Classification

Next, we assessed the degree to which hand kinematics were condition-specific. That is, we gauged the extent to which hand postures were dependent on the object to be grasped or the letter/number to be signed. To this end, we used linear discriminant analysis (LDA) to classify conditions based on the instantaneous hand posture (measured in joint angles) 100-ms before object contact or when the ASL sign had been achieved. Classification performance with the full kinematics provided a ceiling of the achievable classification with LDA.

Next, we gradually removed PCs in descending order of variance by reconstructing the hand posture on each trial based on a progressively smaller subset of PCs. We then used LDA to classify the grasped object or the ASL posture with leave-one-out cross validation. That is, we trained a linear discriminant classifier with the reconstructed hand postures from N-1 randomly selected trials (where N is the total number of trials) and used it to classify the final trial, leaving out each trial on successive iterations. Performance was gauged by the proportion of correct classifications. For the classification based on neuronal data, we computed the spike count of M1 neurons (monkey 1: N = 61; monkey 2: N = 63) over a time window before object contact, the duration of which was optimized for each monkey (100

and 200 ms for monkeys 1 and 2, respectively). As was done with the kinematics, we performed an LDA with leave-one out validation based on the resulting vectors of neuronal spike counts then repeated this procedure as we gradually removed PCs.

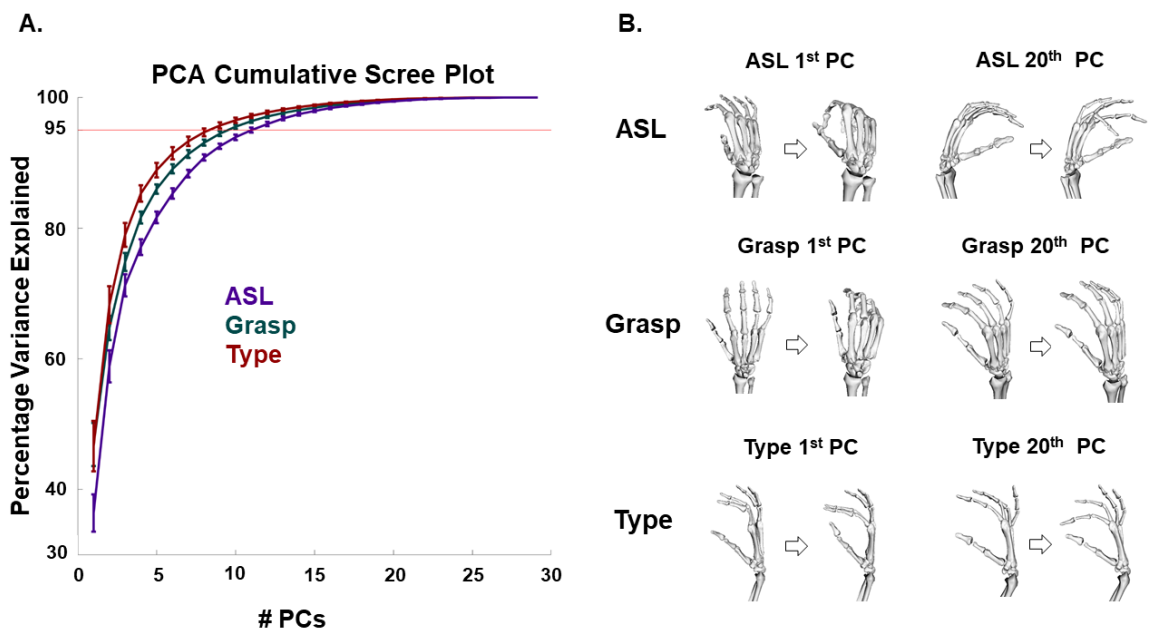

Figure 3. Principal component analysis. A| Cumulative variance plot showing the total percentage of variance explained vs. the number of principal components. PCA is performed separately for each task and subject. The curves are averaged across 8 subjects for grasp and typing and 3 subjects for ASL. B| Visualization of example PCs. For each task, we show the 1st and the 20th PCs (in terms of variance explained). The 20th PC accounts for less than one percent of the variance.

RESULTS

Subjects performed three tasks – grasping various objects, signing the letters of the alphabet in American Sign Language (ASL), and typing two paragraphs on a computer keyboard – while we tracked their hand movements using a camera-based motion tracking system. We wished to examine the degree to which the structure of hand movements was task dependent and differed across individuals. We also wished to ascertain the degree to which hand movements occupy a low-dimensional manifold.

As might be expected, different joint trajectories were observed when subjects grasped different objects or signed different ASL letters (**Figure 2**). Moreover, the kinematics were consistent within condition – grasping a specific object of signing a specific letter – as evidenced by similar trajectories over repeated presentations of the same condition.

Structure of hand kinematics for three manual tasks in humans

First, we wished to reproduce previous findings that much of hand kinematics can be described within a lower dimensional manifold. To this end, we performed a PCA on the joint angles and examined the cumulative variance plot. We found that 3-5 PCs were sufficient to account for 80% of the variance in the kinematics and 8-11 principal components (PCs) accounted for 95% of variance, consistent with

previous findings (**Figure 3A**)[12,35]. We then examined PCs with large and small eigenvalues (**Figure 3B**). In line with previous findings, the first two PCs of grasp and ASL involved opening and closing the hand, engaging mostly metacarpophalangeal (MCP) joint flexion/extension, some proximal and distal interphaleangeal joint flexion/extension (PIP and DIP), and some wrist flexion. One might expect PCs with small eigenvalues to reflect motor or measurement noise and thus be unstructured. Instead, examination of low-variance PCs (the 20th, e.g.) revealed coordinated joint movements (e.g. ring PIP and MCP flexion in ASL, "pinch" flexion in type) that were systematically dependent on condition (**Figure 3B**).

Task- and subject-dependence of the kinematic structure

Next, we compared the subspace of hand kinematics across tasks. To this end, we used a cross-projection similarity measure which gauges the extent to which PCs derived from the kinematics in one task account for the kinematics in the other, and vice-versa [11]. We found that the PC subspaces of all three tasks were more similar than would be expected by chance (two-sample t-test, DOF = 210, p = 9.29e-110) and that the kinematic subspace of ASL and Grasp was similar but differed from the kinematic subspace of typing (two-sample t-test, DOF = 110, *p* =2.58e-05) (**Figure 4A**). We then gauged the degree to which the kinematic subspaces were similar across subjects using the same similarity measure and found that PC subspaces from the same task but different subjects were more similar to each other than were PC subspaces from the same subject but different tasks (paired t-test, *DOF = 56*, *p* = 1.65e-05) (**Figure 4B**). That is, different tasks involve different kinematic structure but that structure is consistent across individuals (cf. [36]).

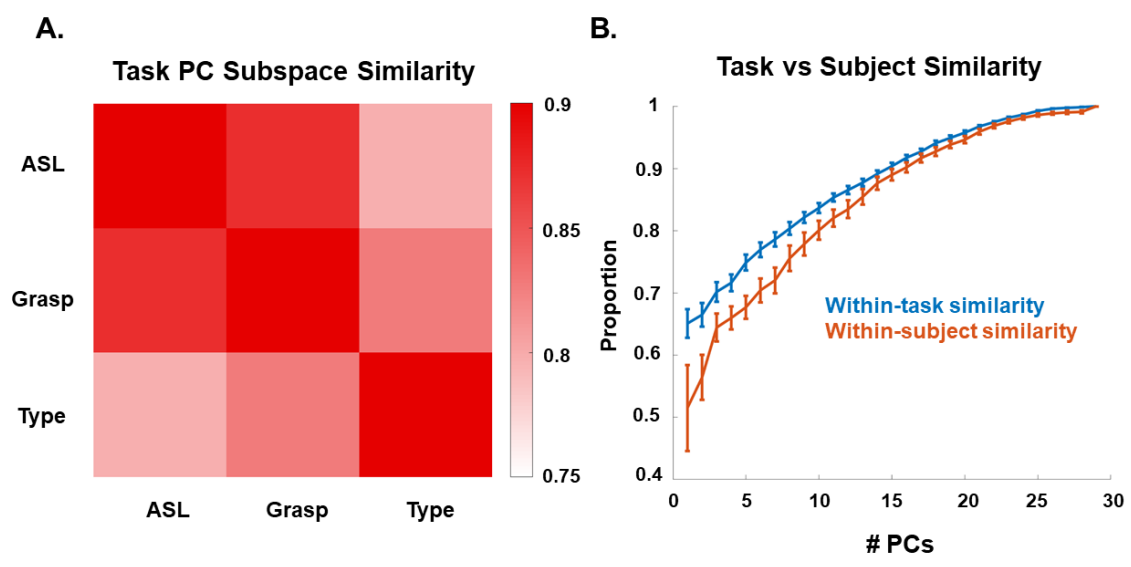

Figure 4. Similarity of kinematic manifolds across tasks and subjects. A| Similarity of the subspaces (formed by the first 10 PCs, accounting for 95% Variance) of pairs of tasks, gauged by cross-projection similarity [42]. ASL and grasp occupy similar manifolds and typing is distinct from these. B| Mean subspace similarity within task/across subjects and the converse. Differences in kinematic manifolds are more pronounced across tasks than they are across subjects.

Structure of low-variance PCs

Having replicated previous results that (1) hand movements can be reconstructed with high precision using a reduced basis set and (2) the resulting synergies are consistent across subjects, we then examined whether the low-variance PCs were structured. We found that the kinematics projected on the low-variance PCs across repeated presentations of the same condition (same grasped object, same ASL letter) varied systematically with the grasped object or signed letter (**Figure 5 A, B**), although this structure was noisier than that in the high-variance PCs, as might be expected (**Figure 5 C, D**). In other words, even the low-variance PCs reflect structure rather than noise in the kinematics. The trajectories along all PCs were far more consistent than would be expected by chance (See **Figure S1**).

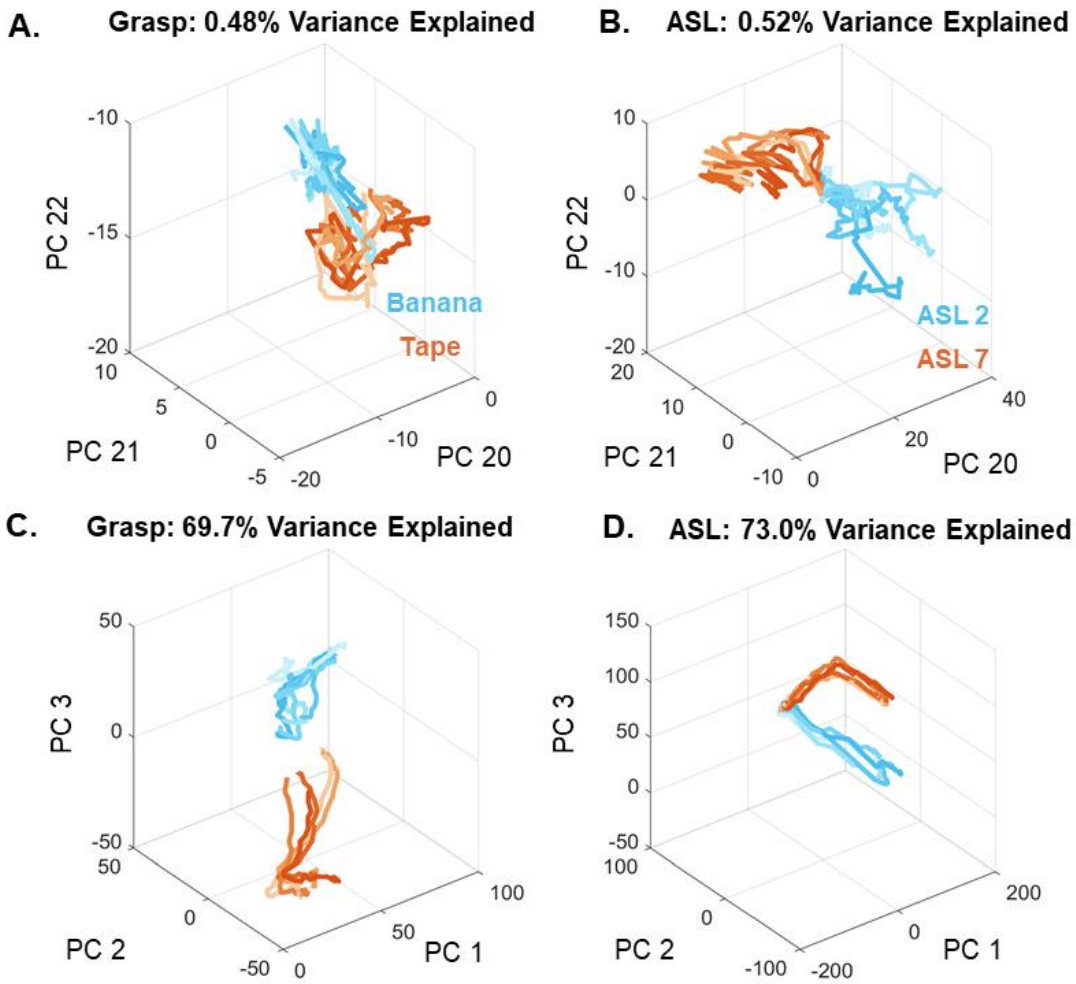

Figure 5. Object-specific kinematics in PC subspaces. A| Projection of the kinematics onto the subspace formed by PCs 21 through 23 for five grasps each of tape and banana. B| Projection of the kinematics for five repeated signs each of "two" and "seven" in ASL onto PCs 21 through 23. C| Projection of the kinematics onto PCs 1 through 3 for the conditions shown in panel A. D| Projection of the kinematics onto PCs 1 through 3 for the conditions shown in panel B. In all panels, separate objects and signs are indicated by color, and different trials are indicated by traces of different brightness.

To quantify the degree to which kinematics differed across conditions, we classified objects or letters

using progressively reduced kinematic subspaces. We found that classification accuracy was above chance even after all but the last few PCs had been removed, and that high performance was achieved even with PCs which collectively accounted for less than one percent of the variance in kinematics (**Figure 6 A, B**). A similar result was obtained when progressively removing LDA dimensions rather than PCs (**Supplementary Figure 2**). Results from these classification analyses are thus inconsistent with the hypothesis that low-variance PCs reflect motor or measurement noise. Rather, these PCs seem to reflect subtle dimensions of movement that are under volitional control and contribute to the exquisitely precise pre-shaping of the hand to an object or to the detailed execution of a complex conformation as is required in ASL.

Structure of hand kinematics during grasp in monkeys

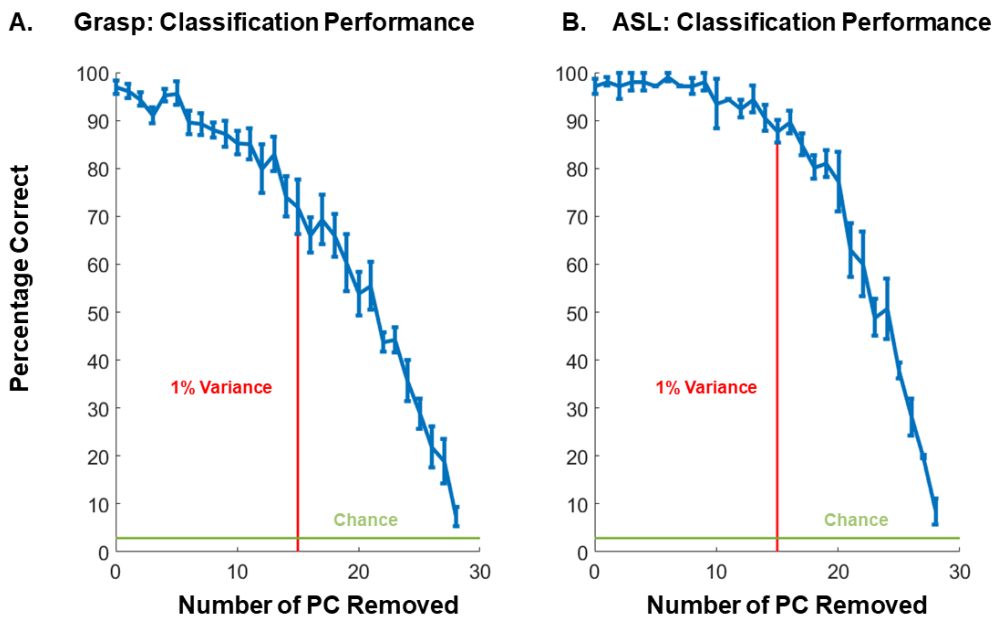

Figure 6. Classification of condition (object, sign) based on kinematics in progressively reduced subspaces. A| Grasp classification performance after progressively removing PCs, from high variance to low. B| ASL classification performance with reduced kinematic subspaces. Vertical lines denote the PC beyond which less than 1% of the variance is accounted for. Note that objects and letters can be classified accurately based on just a handful of high-variance PCs (**Supplementary Figure 4**).

Next, we examined whether the hand kinematics of macaques matched that of humans during grasp. To this end, we tracked the hand movements of two monkeys as they grasped 35 different objects then assessed the dimensionality of their hand kinematics as described above. As was the case with the human hand, low-variance PCs supported classification performance well above chance (**Figure 7 A, B**). In contrast to humans, however, the two animals produced less object specific hand postures, i.e. exhibited a greater tendency to use similar postures for different objects (especially Monkey 2), though this may in part reflect a less diverse set of objects than was used in the human grasp task.

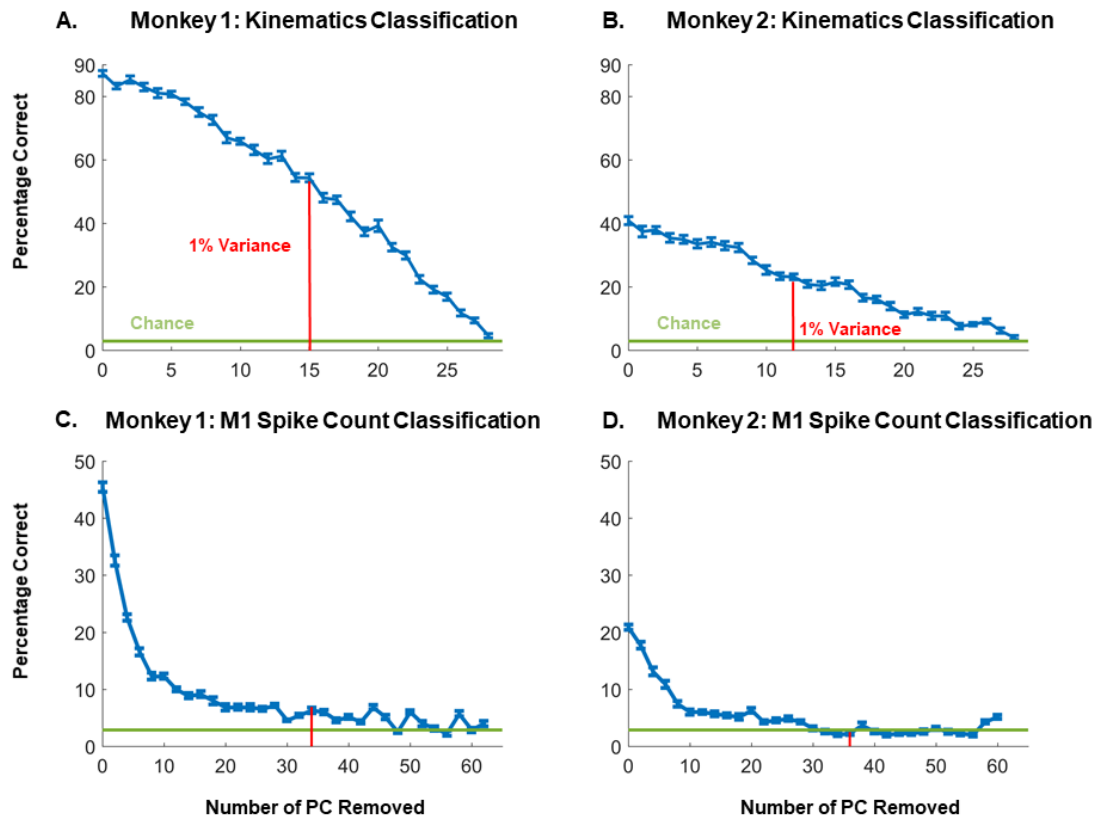

Figure 7. Classification of grasped object based on kinematics and neural responses measured in monkeys. A| Classification performance vs. number of kinematic PCs removed for the two monkeys. B| Classification performance vs. number of neural PCs removed for the two monkeys. We calculated the spike counts of M1 neurons within a short time window before object contact, performed PCA on the responses, and then assessed classification performance with progressively reduced subspaces.

Structure of neuronal representations in sensorimotor cortex during grasp

Time-varying angles of hand joints have been shown to be encoded by neurons in primary motor cortex (M1)[26,37,38] and whole hand posture can be accurately decoded from the responses of populations of M1 neurons [39,40]. With this in mind, we examined the structure of the neural representations underlying grasp to assess the dimensionality of these representations. To this end, we recorded the responses of M1 neurons (Monkey 1: 63 neurons; Monkey 2: 61 neurons) while the two monkeys performed the grasping task. We then attempted to classify grasped objects based on spike counts in M1 and repeated this analysis with progressively reduced neuronal subspaces, as we had done with kinematics. Again, we achieved above chance performance even with dozens of PCs removed (**Figure 7 C, D**). Thus, high-dimensional hand kinematics are accompanied by a high-dimensional neuronal representation of hand posture in M1. Consistent with the hypothesized

relationship between the dimensionality of hand kinematics and that of the underlying neuronal representation, the monkey with the more complex hand kinematics also exhibited the more complex neuronal representation.

DISCUSSION

The structure of hand kinematics depends on the manual behavior

Examination of time-varying human hand postures revealed substantial differences in the structure of the kinematics across some tasks but not others. Specifically, grasping and ASL elicited hand movements with similar patterns of inter-joint correlations whereas typing yielded very different patterns. In fact, the kinematic structure was more similar across subjects than it was across tasks. This result challenges the notion that hand movements are constrained to a universal lower-dimensional manifold regardless of the behavior [9,19,23]. Indeed, ours is only a replication of the finding that different tasks involve different kinematic manifolds [11,12,41].

Volitional hand movements are high dimensional

That the correlational structure of hand movements changes substantially across tasks argues against the hypothesis that hand movements universally occupy some lower dimensional manifold, reflecting a neural strategy to simplify hand control. However, one possibility is that hand movements are low-dimensional within any one task, and that manifold changes from task to task. Indeed, one hypothesis derived from (but not necessarily entailed by) optimal feedback control theory stipulates that the CNS defines low-dimensional manifolds of control to satisfy movement goals on a task-by-task basis, with motor noise being preferentially shunted into dimensions outside of such manifolds [42–44]. According to this hypothesis, the readout of grip type or ASL letter should be restricted to a lower-dimensional manifold than that afforded by the biomechanics of the hand. In other words, even though grasp and ASL spelling occupy a different manifold than does typing, those different manifolds should, themselves, be low-dimensional. However, classification based on subsets of principal components revealed that high-rank (e.g., 20-22) PCs contain substantial object- and ASL sign-specific information. Indeed, kinematic trajectories projected on high-rank PCs were highly consistent within condition and different across conditions (**Supplementary Figure 1**). Such task-relevant information would not be present if such dimensions simply reflected motor or measurement noises, suggesting instead that volitionally controlled hand movements occupy a high dimensional space.

High dimensional neuronal representation reflect a complex control scheme

Consistent with their human counterparts, the grasp kinematics in rhesus macaques were found to be high dimensional, as evidenced by the fact that trajectories along low-variance PCs were highly object dependent. In light of this, we examined whether the underlying cortical representations might be similarly high-dimensional. Previous work to date [45–48] has suggested that activity in primary motor cortex (M1) operates primarily within a low-dimensional manifold that may reflect volitional control of specific movement synergies [13,15]. However, studies of M1 structure are often constrained to a low-dimensional task, e.g. reaching, which limits the apparent dimensionality of the M1 representation [49]. The neuronal activity evoked as monkeys performed a high dimensional manual task spanned a high-dimensional space. Indeed, as with the kinematics, both low-rank and high-rank

PCs of neural activity carried object-specific information. In other words, the volitional control of grasp is high-dimensional and is supported by patterns of neural activity in M1 that occupy a high-dimensional space.

Implications for the interpretation of synergies

High-dimensional kinematics do not imply wholly unconstrained control of the hand. Indeed, single-finger movements attempted by monkeys [50] and humans [51] are never perfectly individuated: They comprise incidental movements of the other digits arising in part from co-contraction of musculature associated with other digits. Moreover, despite its potential for high-dimensional activity patterns, volitional control of patterns of M1 activity does not extend to all arbitrary co-activations among neurons [45]. Rather, our results imply that the dimensionalities spanned by volitional hand movements and associated patterns of M1 activity are higher than one might expect if the neural control of hand postures were reduced to a low-dimensional manifold, either universally or on a task-by-task basis, as a means to simplify the control problem. Moreover, the degree to which volitional movements of the hand are high dimensional relative to those of other effectors has been documented previously [16,52–54] and is perhaps enabled by the abundance of specialized corticomotoneuronal projections from M1 to hand-related muscles in primates [6]. As such, our results are consistent with a specialized high-dimensional neural control strategy for the hand, indicating a different role (object manipulation) than that of other effectors.

Recent advances in large scale recordings of neuronal activity suggest that the notion that the nervous system would need to simplify manual control is fundamentally misguided. Indeed, sensory representations of natural scenes in primary visual cortex (V1) eclipse 500 dimensions [55], an order of magnitude more than the implied representations of hand postures. Nonetheless, visual percepts are highly intuitive and complex objects can be identified accurately, rapidly, and effortlessly [56]. In comparison, motor control is positively simple!

REFERENCES

1. Elkoura G, Singh K. Handrix: animating the human hand. SIGGRAPH Symp Comput Animat. 2003; doi:10.1016/0006-3002(57)90271-8

2. Lee JC, Healy FJC. Anatomy of the Wrist and Hand. Radiographics. 2005; doi:10.1148/rg.256055028

3. Johnson K. The roles and functions of cutaneous mechanoreceptors. Curr Opin Neurobiol. 2001;11: 455–461. doi:10.1016/S0959-4388(00)00234-8

4. Sur M, Merzenich MM, Kaas JH. Magnification, receptive-field area, and "hypercolumn" size in areas 3b and 1 of somatosensory cortex in owl monkeys. J Neurophysiol. 1980;44: 295–311. doi:10.1152/jn.1980.44.2.295

5. Schieber MH. Constraints on Somatotopic Organization in the Primary Motor Cortex. J Neurophysiol. 2001;86: 2125–2143. doi:10.1152/jn.2001.86.5.2125

6. Rathelot J-A, Strick PL. Subdivisions of primary motor cortex based on cortico-motoneuronal

cells. Proc Natl Acad Sci. 2009;106: 918–923. doi:10.1073/pnas.0808362106

7. Bernstein NA. The co-ordination and regulation of movements: Conclusions towards the Study of Motor Co-ordination. Biodynamics of Locomotion. 1967. doi:10.1097/00005072-196804000-00011

8. Flash T, Hochner B. Motor primitives in vertebrates and invertebrates. Current Opinion in Neurobiology. 2005. doi:10.1016/j.conb.2005.10.011

9. Tresch MC, Jarc A. The case for and against muscle synergies. Curr Opin Neurobiol. 2009;19: 601–607. doi:10.1016/j.conb.2009.09.002

10. Santello M, Bianchi M, Gabiccini M, Ricciardi E, Salvietti G, Prattichizzo D, et al. Hand synergies: Integration of robotics and neuroscience for understanding the control of biological and artificial hands. Physics of Life Reviews. 2016. doi:10.1016/j.plrev.2016.02.001

11. E. Todorov, Z. Ghahramani. Analysis of the synergies underlying complex hand manipulation. Proc 26th Annu Int Conf IEEE EMBS. 2004; doi:10.1109/iembs.2004.1404285

12. Ingram JN, Körding KP, Howard IS, Wolpert DM. The statistics of natural hand movements. Exp Brain Res. 2008;188: 223–236. doi:10.1007/s00221-008-1355-3

13. Overduin SA, d'Avella A, Carmena JM, Bizzi E. Microstimulation Activates a Handful of Muscle Synergies. Neuron. Elsevier Inc.; 2012;76: 1071–1077. doi:10.1016/j.neuron.2012.10.018

14. Overduin SA, d'Avella A, Roh J, Bizzi E. Modulation of muscle synergy recruitment in primate grasping. J Neurosci. Society for Neuroscience; 2008;28: 880–92. doi:10.1523/JNEUROSCI.2869-07.2008

15. Overduin SA, d'Avella A, Roh J, Carmena JM, Bizzi E. Representation of Muscle Synergies in the Primate Brain. J Neurosci. Society for Neuroscience; 2015;35: 12615–12624. doi:10.1523/JNEUROSCI.4302-14.2015

16. Valero-Cuevas FJ, Venkadesan M, Todorov E. Structured Variability of Muscle Activations Supports the Minimal Intervention Principle of Motor Control. J Neurophysiol. 2009; doi:10.1152/jn.90324.2008

17. Kutch JJ, Valero-Cuevas FJ. Challenges and new approaches to proving the existence of muscle synergies of neural origin. PLoS Comput Biol. 2012;8. doi:10.1371/journal.pcbi.1002434

18. Kutch JJ, Kuo AD, Bloch AM, Rymer WZ. Endpoint Force Fluctuations Reveal Flexible Rather Than Synergistic Patterns of Muscle Cooperation. J Neurophysiol. 2008; doi:10.1152/jn.90274.2008

19. Santello M, Soechting JF. Gradual molding of the hand to object contours. J Neurophysiol. 1998;79: 1307–1320. doi:papers2://publication/uuid/A2B015E6-8AE1-4A49-ACE2-9042E4BE8C17

20. Tresch MC. Matrix Factorization Algorithms for the Identification of Muscle Synergies:

Evaluation on Simulated and Experimental Data Sets. J Neurophysiol. 2005;95: 2199–2212. doi:10.1152/jn.00222.2005

21. Furuya S, Flanders M, Soechting JF. Hand kinematics of piano playing. J Neurophysiol. 2011;106: 2849–2864. doi:10.1152/jn.00378.2011

22. Patel V, Burns M. Linear and Nonlinear Kinematic Synergies in the Grasping Hand. J Bioeng Biomed Sci. 2015; doi:10.4172/2155-9538.1000163

23. Santello M, Flanders M, Soechting JF. Postural Hand Synergies for Tool Use. J Neurosci. 1998;18: 10105–10115. doi:10.1523/JNEUROSCI.18-23-10105.1998

24. Rajagopal A, Dembia CL, DeMers MS, Delp DD, Hicks JL, Delp SL. Full-Body Musculoskeletal Model for Muscle-Driven Simulation of Human Gait. IEEE Trans Biomed Eng. 2016; doi:10.1109/TBME.2016.2586891

25. Delp SL, Anderson FC, Arnold AS, Loan P, Habib A, John CT, et al. OpenSim: Open-source software to create and analyze dynamic simulations of movement. IEEE Trans Biomed Eng. 2007; doi:10.1109/TBME.2007.901024

26. Goodman JM, Tabot GA, Lee AS, Suresh AK, Rajan AT, Hatsopoulos NG, et al. Postural representations of the hand in primate sensorimotor cortex. bioRxiv. 2019; 566539. doi:10.1101/566539

27. Anderson FC, Pandy MG. Dynamic Optimization of Human Walking. J Biomech Eng. American Society of Mechanical Engineers; 2001;123: 381–390. doi:10.1115/1.1392310

28. Anderson FC, Pandy MG. A Dynamic Optimization Solution for Vertical Jumping in Three Dimensions. Comput Methods Biomech Biomed Engin. 1999;2: 201–231. doi:10.1080/10255849908907988

29. Delp SL, Loan JP, Hoy MG, Zajac FE, Topp EL, Rosen JM. An interactive graphics-based model of the lower extremity to study orthopaedic surgical procedures. IEEE Trans Biomed Eng. 1990;37: 757–767. doi:10.1109/10.102791

30. Dempster WT, Gaughran GRL. Properties of body segments based on size and weight. Am J Anat. 1967;120: 33–54. doi:10.1002/aja.1001200104

31. Holzbaur KRS, Murray WM, Delp SL. A Model of the Upper Extremity for Simulating Musculoskeletal Surgery and Analyzing Neuromuscular Control. Ann Biomed Eng. 2005;33: 829–840. doi:10.1007/s10439-005-3320-7

32. Yamaguchi GT, Zajac FE. A planar model of the knee joint to characterize the knee extensor mechanism. J Biomech. 1989;22: 1–10.

33. de Leva P. Adjustments to Zatsiorsky-Seluyanov's segment inertia parameters. J Biomech. 1996;29: 1223–30.

34. Ringnér M. What is principal component analysis? Nat Biotechnol. 2008;26: 303–304. doi:10.1038/nbt0308-303

35. Thakur PH, Bastian AJ, Hsiao SS. Multidigit Movement Synergies of the Human Hand in an Unconstrained Haptic Exploration Task. J Neurosci. 2008;28: 1271–1281. doi:10.1523/JNEUROSCI.4512-07.2008

36. Todorov E, Ghahramani Z. Analysis of the synergies underlying complex hand manipulation. 2005. pp. 4637–4640. doi:10.1109/iembs.2004.1404285

37. Saleh M, Takahashi K, Amit Y, Hatsopoulos NG. Encoding of coordinated grasp trajectories in primary motor cortex. J Neurosci. 2010;30: 17079–90. doi:10.1523/JNEUROSCI.2558-10.2010

38. Saleh M, Takahashi K, Hatsopoulos NG. Encoding of coordinated reach and grasp trajectories in primary motor cortex. J Neurosci. 2012;32: 1220–32. doi:10.1523/JNEUROSCI.2438-11.2012

39. Okorokova E V., Goodman JM, Hatsopoulos NG, Bensmaia SJ. Decoding hand kinematics from population responses in sensorimotor cortex during grasping. 2019;

40. Menz VK, Schaffelhofer S, Scherberger H. Representation of continuous hand and arm movements in macaque areas M1, F5, and AIP: a comparative decoding study. J Neural Eng. 2015;12: 56016. doi:10.1088/1741-2560/12/5/056016

41. Liu D, Todorov E. Evidence for the Flexible Sensorimotor Strategies Predicted by Optimal Feedback Control. J Neurosci. 2007;27: 9354–9368. doi:10.1523/jneurosci.1110-06.2007

42. Todorov E, Jordan MI. Optimal feedback control as a theory of motor coordination. Nat Neurosci. 2002;5: 1226–1235. doi:10.1038/nn963

43. Todorov E. Optimality principles in sensorimotor control. Nature Neuroscience. 2004. doi:10.1038/nn1309

44. Scott SH. Optimal feedback control and the neural basis of volitional motor control. Nat Rev Neurosci. 2004;5: 532–545. doi:10.1038/nrn1427

45. Sadtler PT, Quick KM, Golub MD, Chase SM, Ryu SI, Tyler-Kabara EC, et al. Neural constraints on learning. Nature. 2014;512: 423–426. doi:10.1038/nature13665

46. Gallego JA, Perich MG, Miller LE, Solla SA. Neural Manifolds for the Control of Movement. Neuron. 2017. doi:10.1016/j.neuron.2017.05.025

47. Churchland MM, Cunningham JP, Kaufman MT, Foster JD, Nuyujukian P, Ryu SI, et al. Neural population dynamics during reaching. Nature. Nature Publishing Group; 2012;487: 51–56. doi:10.1038/nature11129

48. Gao P, Ganguli S. On simplicity and complexity in the brave new world of large-scale neuroscience. Curr Opin Neurobiol. Elsevier Ltd; 2015;32: 148–155. doi:10.1016/j.conb.2015.04.003

49. Gao P, Trautmann E, Yu BM, Santhanam G, Ryu SI, Shenoy K V., et al. A theory of multineuronal dimensionality, dynamics and measurement. bioRxiv. 2017; 214262. doi:10.1101/214262

50. Schieber MH. Muscular Production of Individuated Extrinsic Finger Muscles Finger Movements. J Neurosci. 1995;15: 284–297. doi:10.1523/JNEUROSCI.15-01-00284.1995

51. Häger-Ross C, Schieber MH. Quantifying the independence of human finger movements: comparisons of digits, hands, and movement frequencies. J Neurosci. 2000;20: 8542–50. Available: http://www.ncbi.nlm.nih.gov/pubmed/11069962

52. Rácz K, Brown D, Valero-Cuevas FJ. An involuntary stereotypical grasp tendency pervades voluntary dynamic multifinger manipulation. J Neurophysiol. American Physiological Society Bethesda, MD; 2012;108: 2896–2911. doi:10.1152/jn.00297.2012

53. Valero-Cuevas FJ, Yi JW, Brown D, McNamara R V., Paul C, Lipson H. The tendon network of the fingers performs anatomical computation at a macroscopic scale. IEEE Trans Biomed Eng. 2007;54: 1161–1166. doi:10.1109/TBME.2006.889200

54. Santos VJ, Valero-cuevas FJ. Reported Anatomical Variability Naturally Leads to Multimodal Distributions of Denavit-Hartenberg Parameters for the Human Thumb. IEEE Trans Biomed Eng. 2006;53: 155–163. Available: http://www.ncbi.nlm.nih.gov/pubmed/16485744

55. Stringer C, Pachitariu M, Steinmetz N, Carandini M, Harris KD. High-dimensional geometry of population responses in visual cortex. Nature. 2019; doi:10.1038/s41586-019-1346-5

56. Potter MC. Short-Term Conceptual Memory for Pictures. J Exp Psychol Hum Percept Perform. 1976;2: 509–522.

SUPPLEMENTARY FIGURE

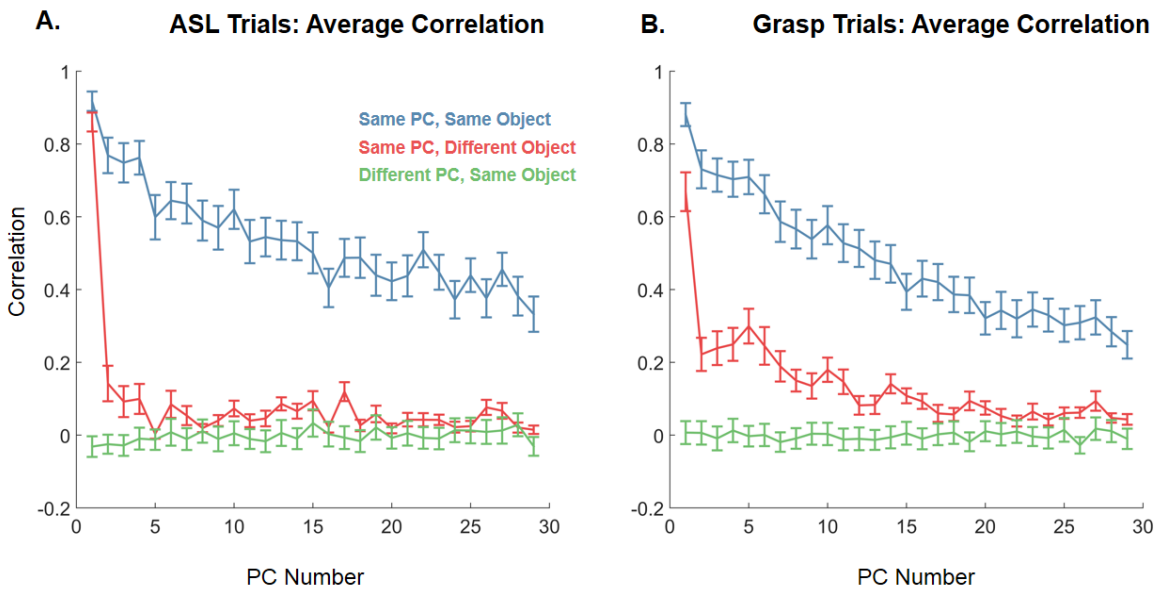

Supplementary Figure 1 Consistency of kinematics projected onto each PC. A| Mean correlation coefficient between kinematics for different trials of the same object projected onto the same PC (blue), for different trials of the same object projected onto different PCs (green), and for trials from different objects projected onto the same PCs (red). The within-object, within-PC correlations are systematically higher than their shuffled counterparts. B| Same analysis for ASL trials.

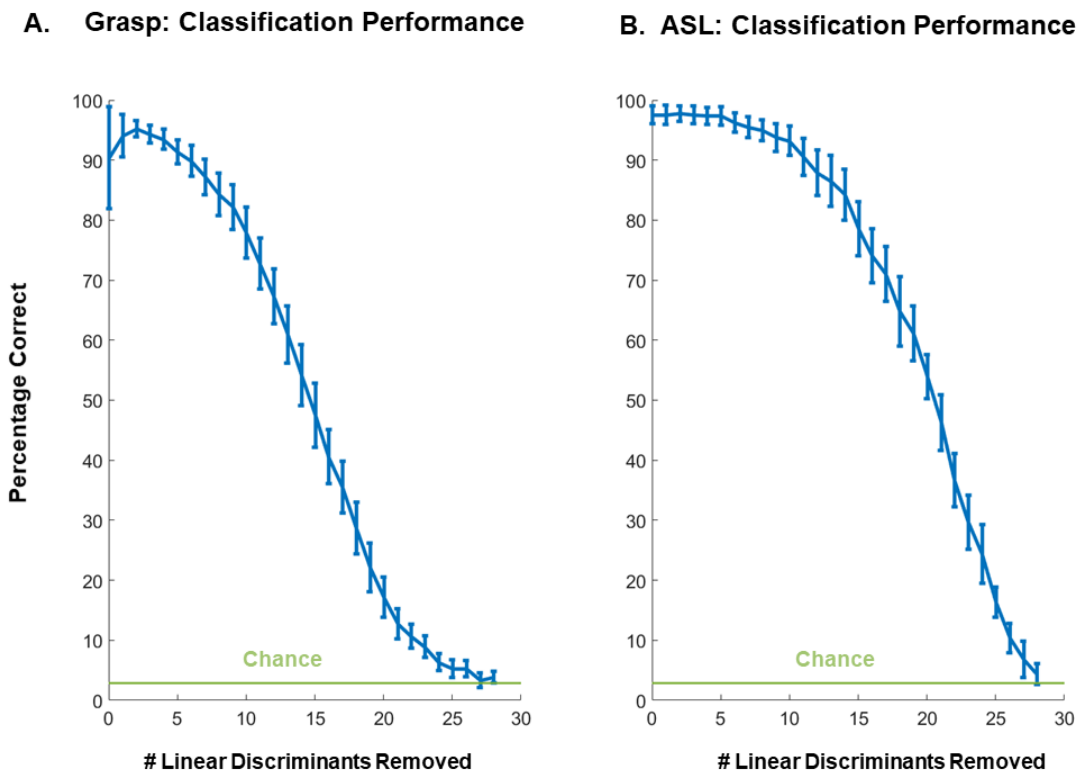

Supplementary Figure 2 Classification *p*erformance with *a progressively reduced number of* linear discriminants. A| Classification accuracy *for* grasped objects as the dimensions identified by LDA were removed *based on their respective* Fisher's coefficient (ratio of between class variance to within class variance)*, from highest* to lowest. B| Classification accuracy of ASL posture as LDA dimensions are removed in the same way.

A. Passage 1: Right Hand Words

lumpy humpy imply nigh jupon ovum; hoping goblin logy limn boil kiln phonily moping plumy junk limb, jumpily lion hump jump moving; knob humping holing homily' bony plum hominy boing ugly buoying puny hunky bulking' juking glim; joking uplink bilgy gonium holy gumbo limo bough mingy milky long young linkup; hymn hypo jumping.

globin loving kilo' bulky plink upon nymph numb moil homing punk; buoy gulp gimpy poky blip humbly honky plough goby ping; gluon bunko gunk yolk inly plying vying bilk opium login bung? Hulky glop ploy plonk king bumping, jumpy glyph bulgy.

Milk monk john bogy yogh, gunky liny plumb glum hunk, ignobly bigly pong bumpy jingo poking lying blink nobly? Lump khoum. Vino lymph phylum joying blog unholy pink junky jokily glom hulking' only bulk pylon milo moly hilum gink poly; bunk join bluing oily yoni ling nimbly unhip. Lough knop puling limy hokum vinyl limp; viol bijou bump bonk buying pony plunk; honk blimp numbly plug' umbo nympho glob.

Bumpkin lumping pinkly hypoing' loping, lubing gumboil jingly holm link pokily, umping muni, lungi bingo hulk kingly, oink mogul impugn pinky hung gimp, pigmy ghoul lung hyping. Phony jumbo pluming; yoking loin bumpily limbo linkboy.

B. Passage 2: Normal Words

The neocortex, also called the neopallium and isocortex, is the part of the mammalian brain involved in higher-order brain functions such as sensory peas sensory perception, cognition and generation of motor commands, spatial reasoning and language. The neocortex contains both excitatory (~80%) and inhibitory (~20%) neurons, named for their effect on other neurons.

The structure of the neocortex is relatively uniform (hence the alternative names "iso-" and "homotypic" cortex), consisting of six horizontal layers segregated principally by cell type and neuronal connections. However, there are many exceptions to this uniformity; for example, layer IV is small or missing in primary motor cortex.

There is some canonical circuitry within the cortex; for example, pyramidal neurons in the upper layers II and III project their axons to other areas of neocortex, while those in the deeper layers V and VI often project out of the cortex, e.g. to the thalamus, brainstem, and spinal cord.

Neurons in layer IV receive the majority of the synaptic connections from outside the cortex (mostly from thalamus), and themselves make short-range, local connections to other cortical layers. Thus, layer IV is the main recipient of incoming sensory information and distributes it to the other layers for further processing.

Supplementary Figure 3 Texts that subject typed during the typing task. A| a collection of words that only used letters to the right of the “Y-G-B” boundary on an English keyboard. Words are arranged in paragraph-like structure with punctuations. B| A passage taken from the Wikipedia page of neocortex (https://en.wikipedia.org/wiki/Neocortex) which used a variety of common and uncommon words.

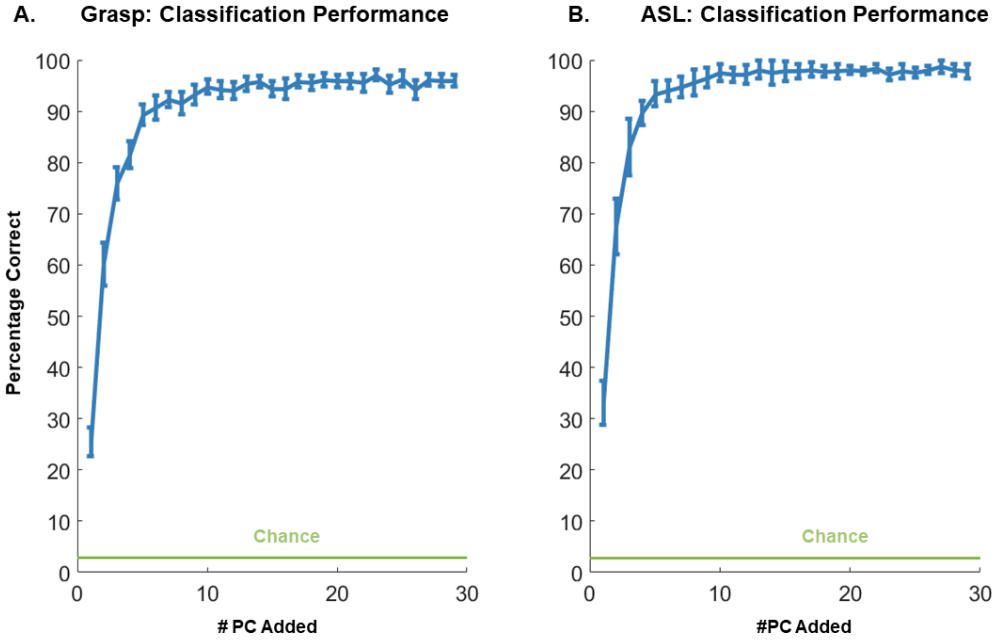

Supplementary Figure 4. Classification performance with progressively larger subspaces. A| Classification performance for grasped objects as PCs are added in descending order of variance explained (blue curve). B| Classification performance for ASL letters vs. number of PCs. Green line denotes chance performance.